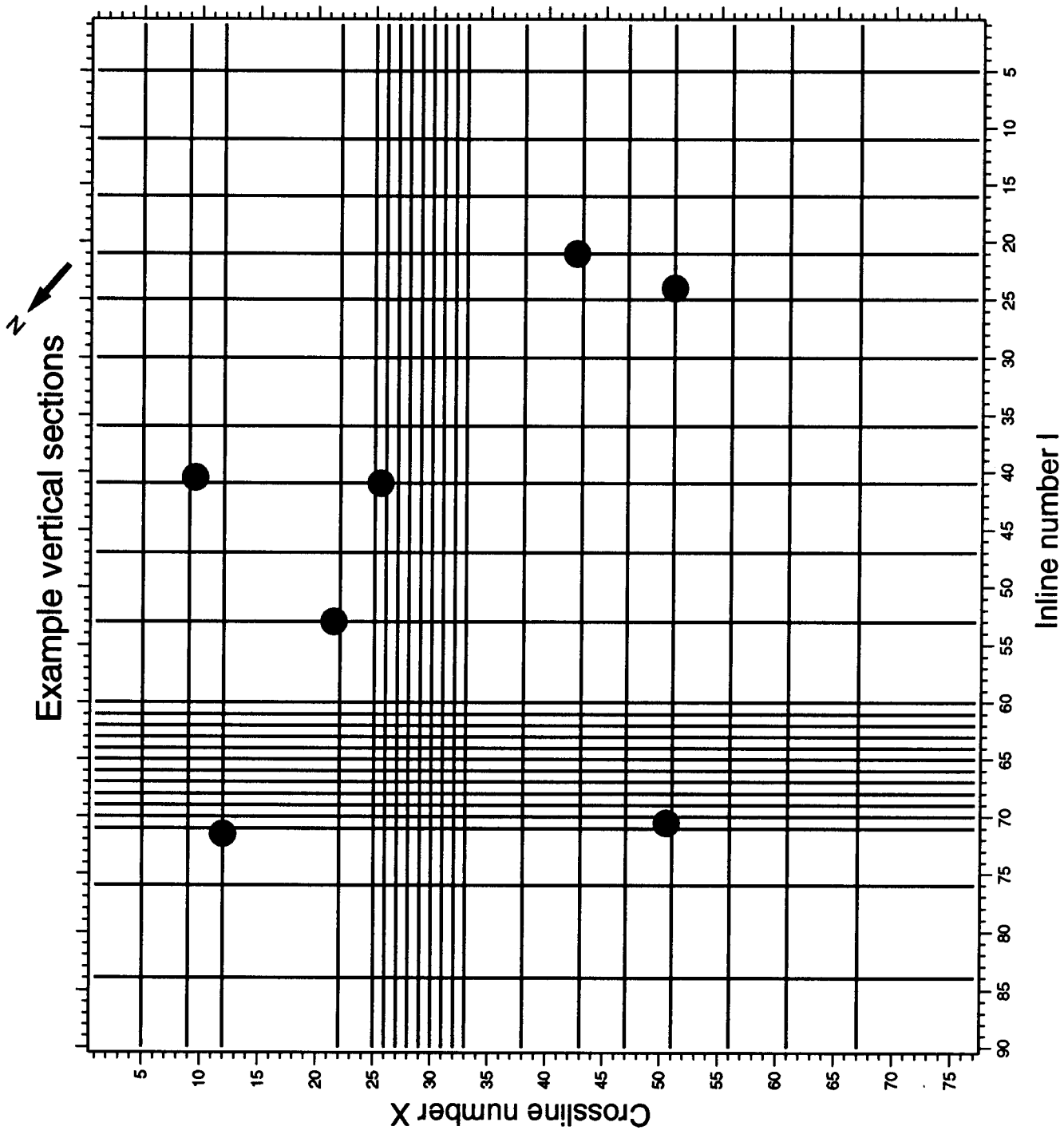

Figure 51. Location map of the full-scale vertical sections in Enclosures.

Note: Principal wells are shown as discs.

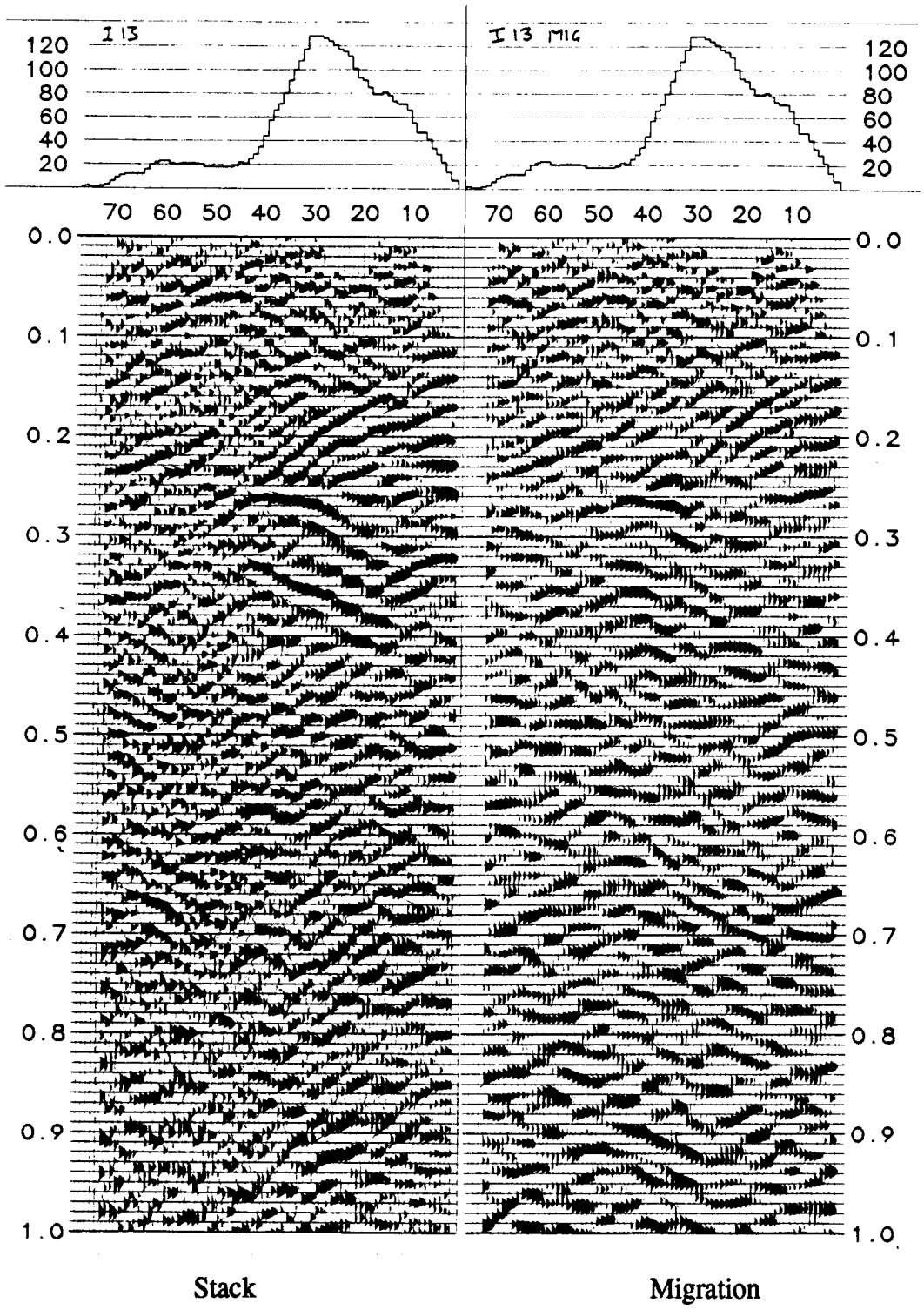

Figure 52. Stacked and migrated displays of inline I13.

Note: Fold of cover is shown graphically at the top.

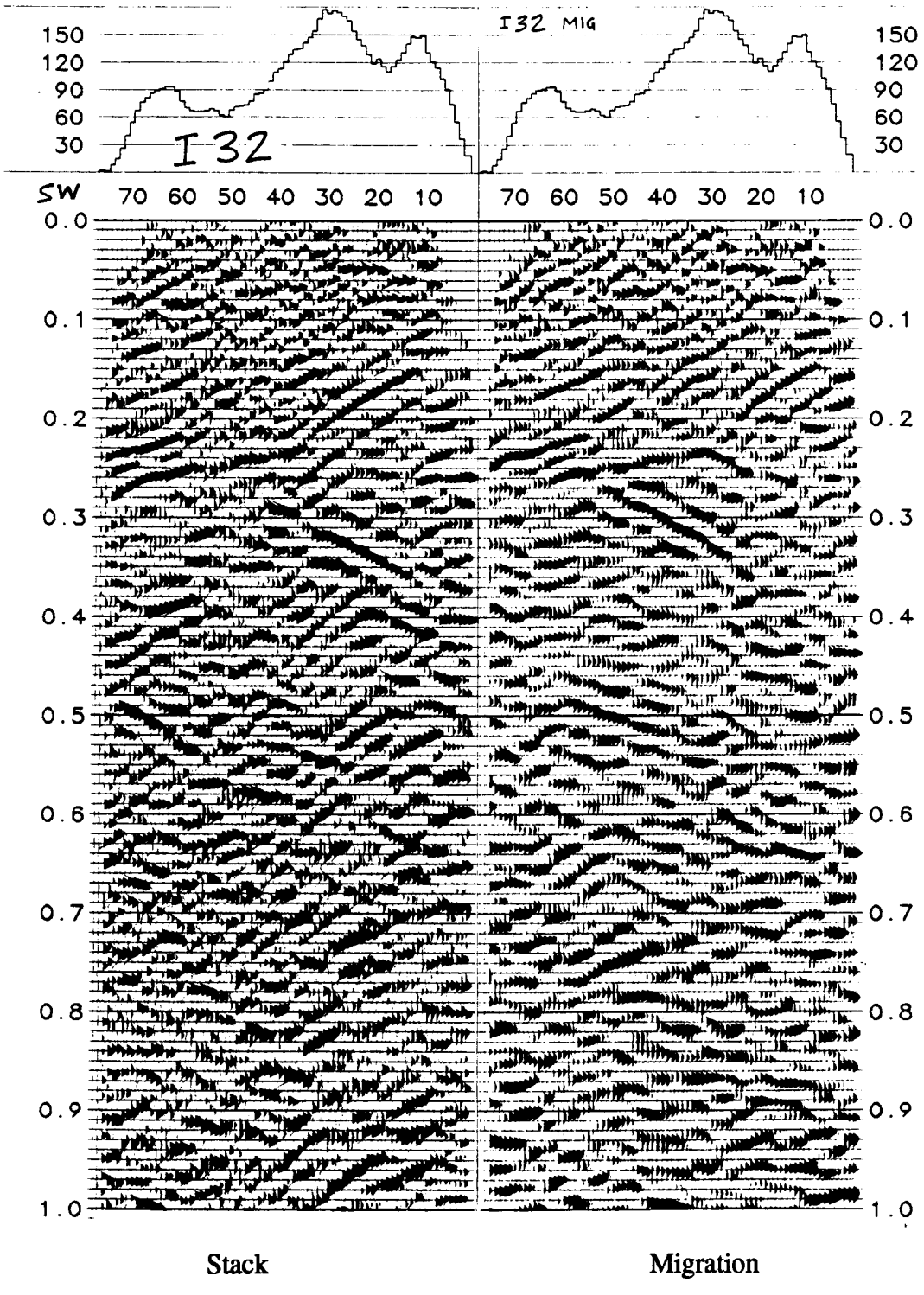

Figure 53. Stacked and migrated displays of inline I32.

Note: Fold of cover is shown graphically at the top.

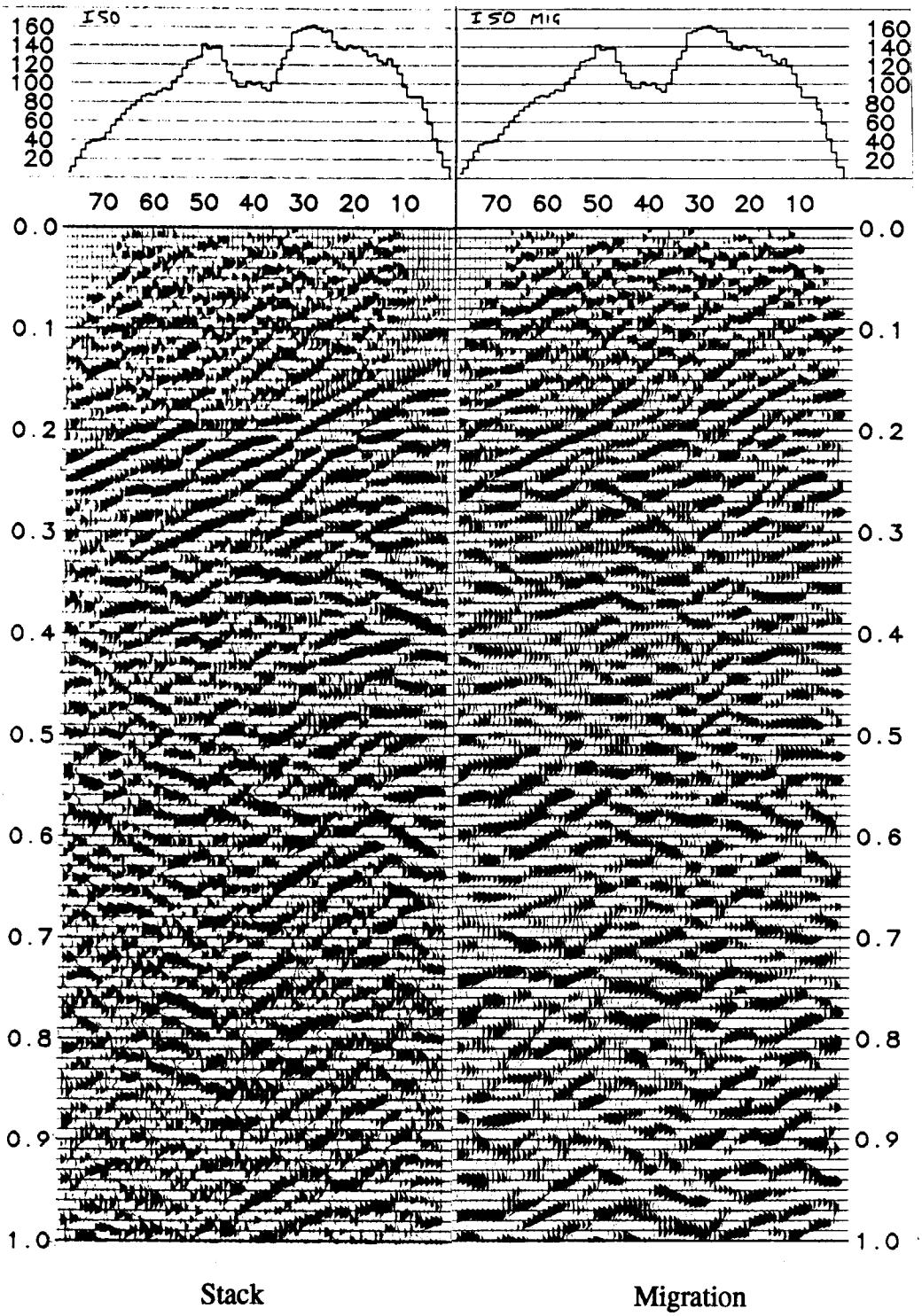

Figure 54. Stacked and migrated displays of inline I50.

Note: Fold of cover is shown graphically at the top.

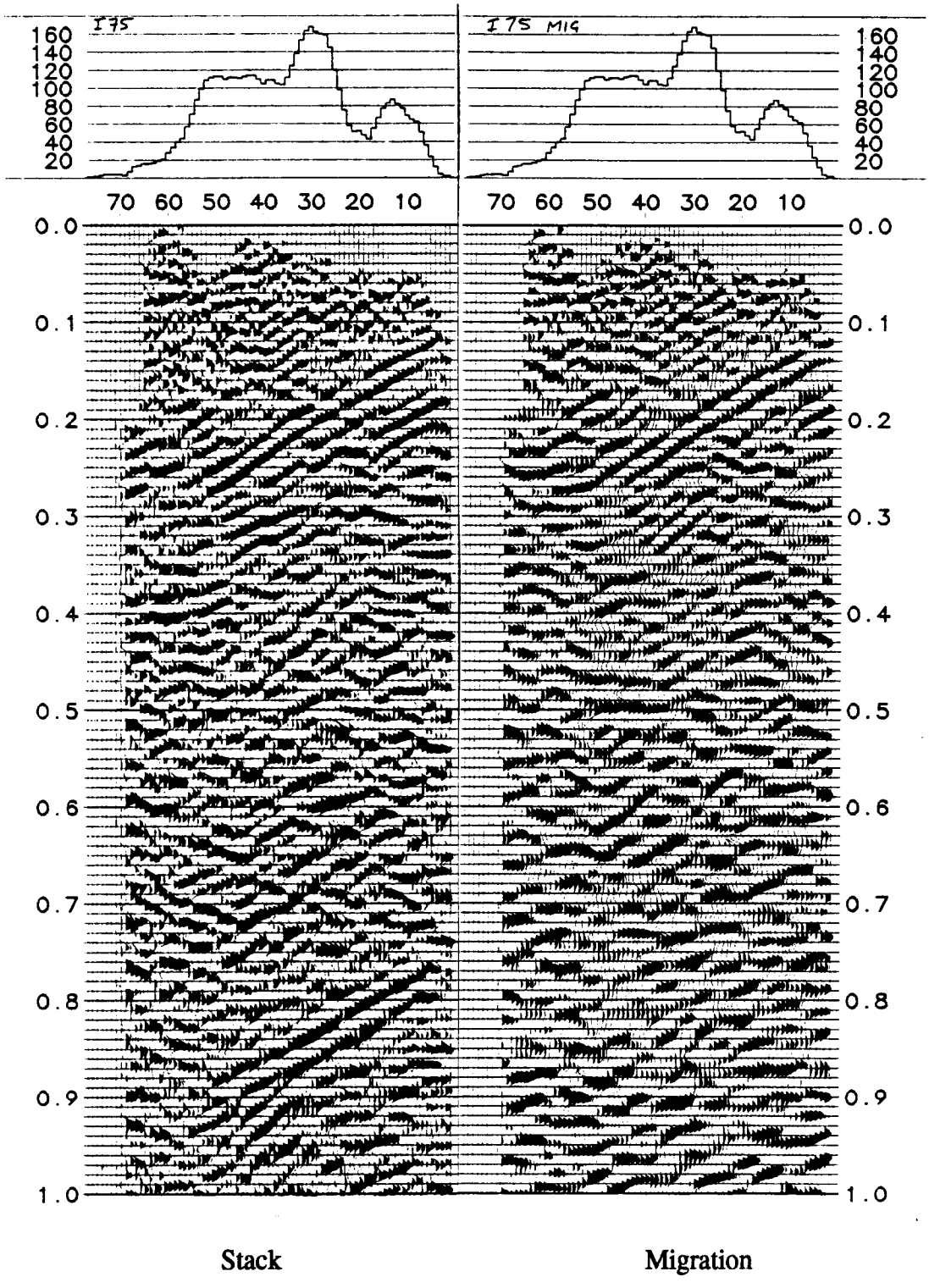

Figure 55. Stacked and migrated displays of inline I75.

Note: Fold of cover is shown graphically at the top.

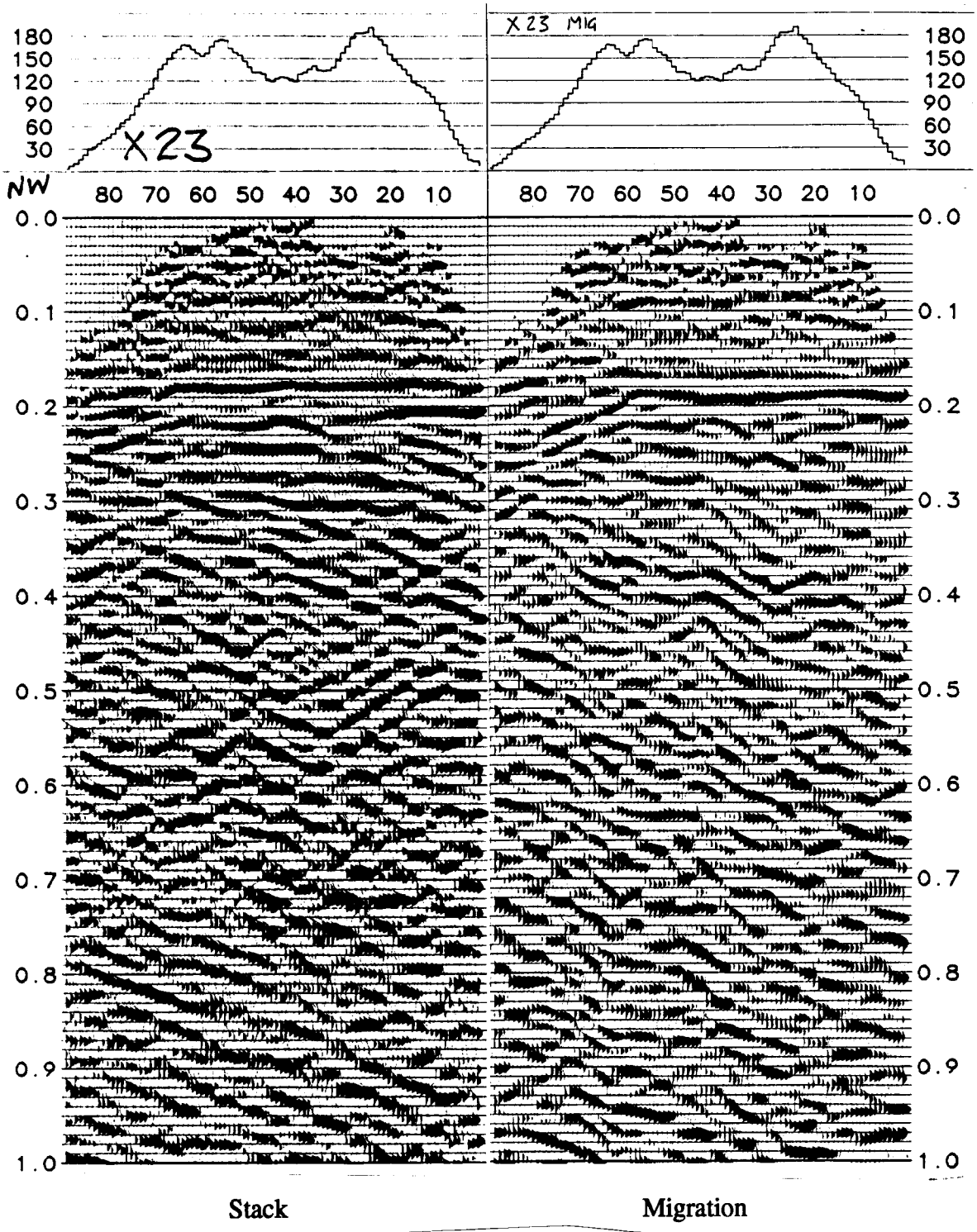

Figure 56. Stacked and migrated displays of crossline X23.

Note: Fold of cover is shown graphically at the top.

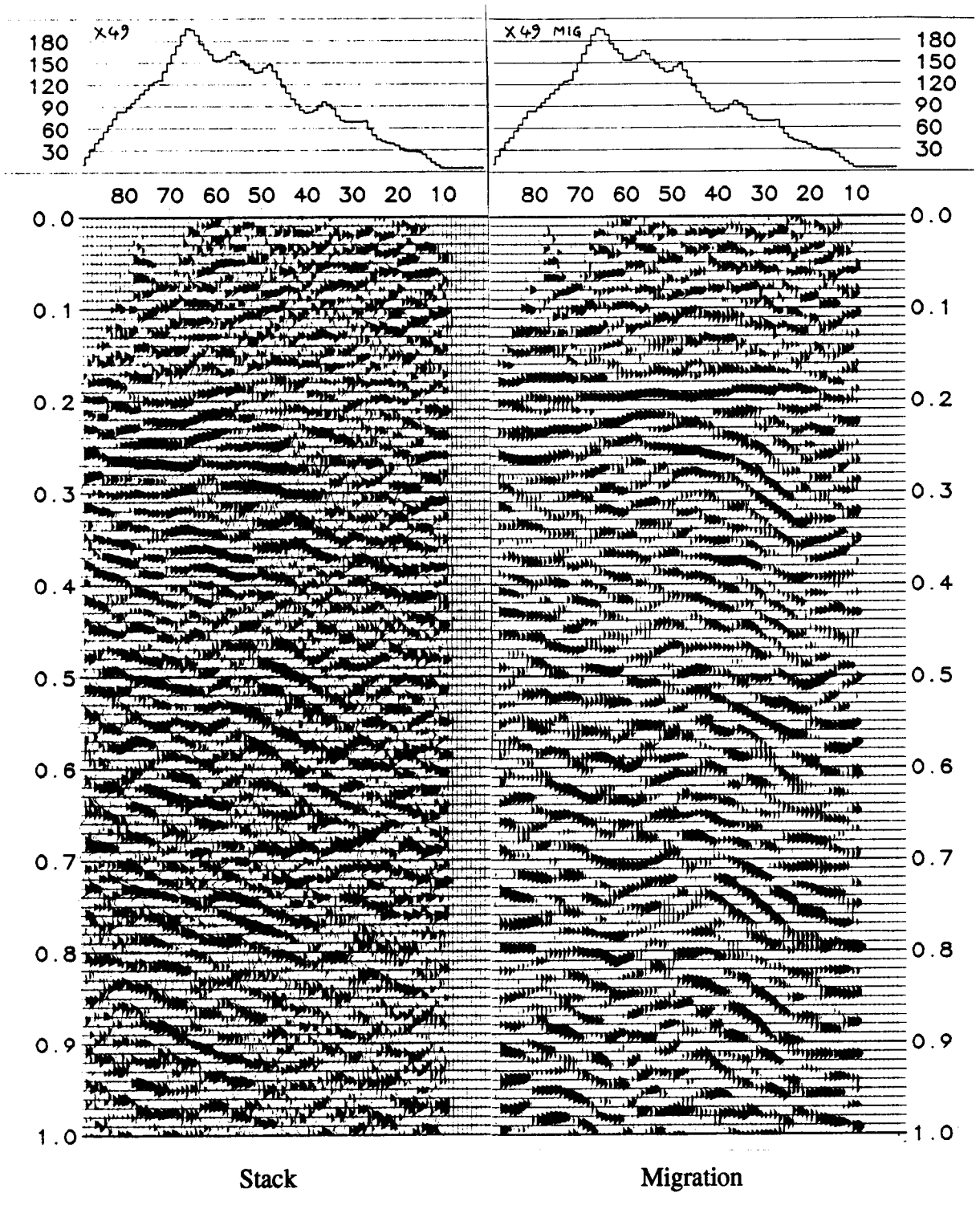

Figure 57. Stacked and migrated displays of crossline X49.

Note: Fold of cover is shown graphically at the top.

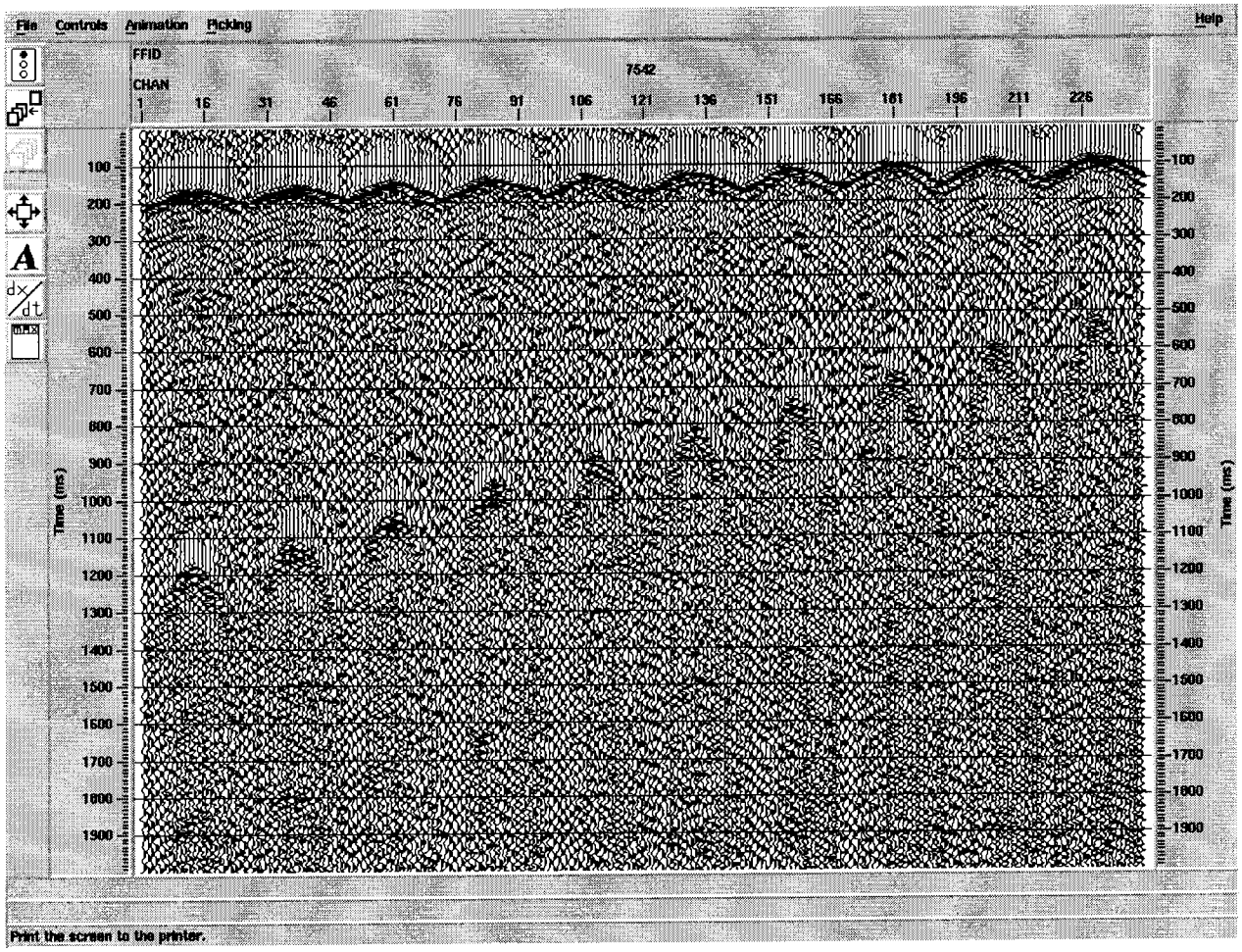

Figure 58. Shot gather from a single sweep.

Note: The prominent first breaks show how the spread (swath B2) is divided into 10 rows of 24 channels each, with the source to the north-east (VP 3635; 1 vibrator). A 200 ms centred AGC has been applied. Time scale is 0-600 ms.

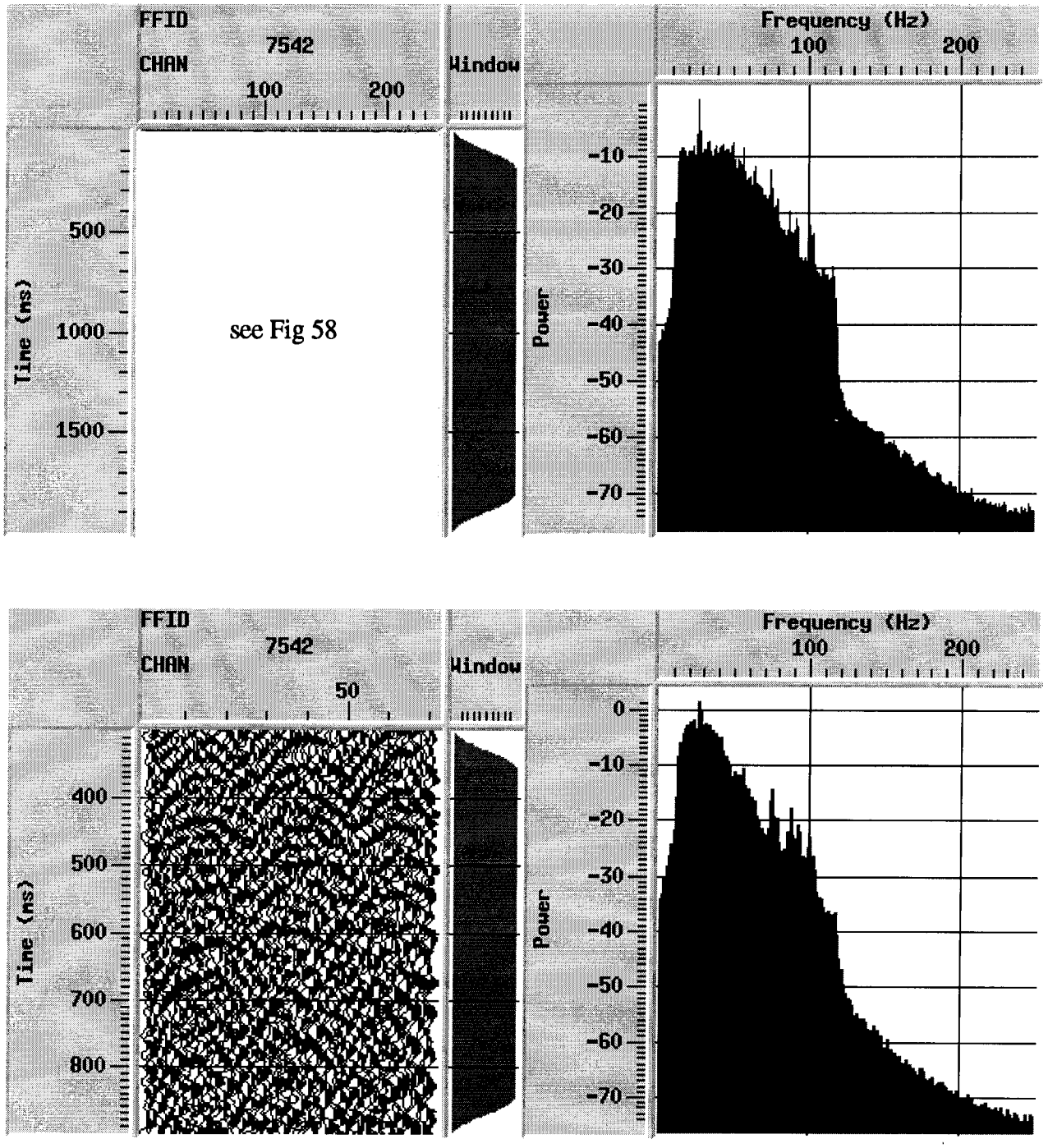

Figure 59. Panels from Figure 58 with corresponding power spectrum.

Note: Hanning window for the traces is shown in the centre. Upper row is the whole panel from Figure 58; lower display is a window of the same data containing some reflections. Note the pronounced increase in the power spectrum within the band 12-120 Hz. The spike at 25 Hz is due to environmental (mechanical) noise seen clearly at the left-hand side of Figure 58.

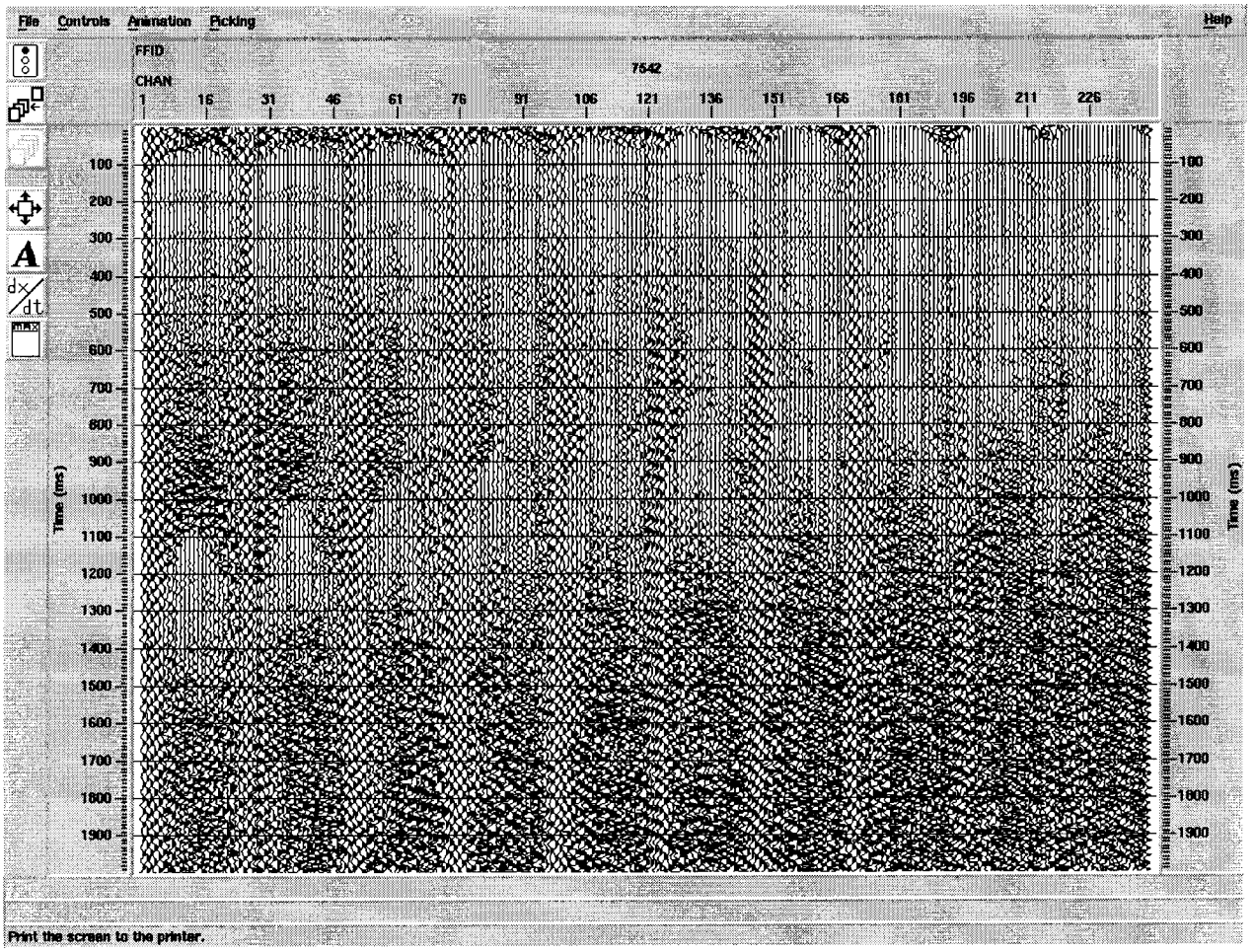

Figure 60. Subtraction record corresponding to Figure 58.

Note: One sweep has been subtracted from another to leave non-signal generated noise.

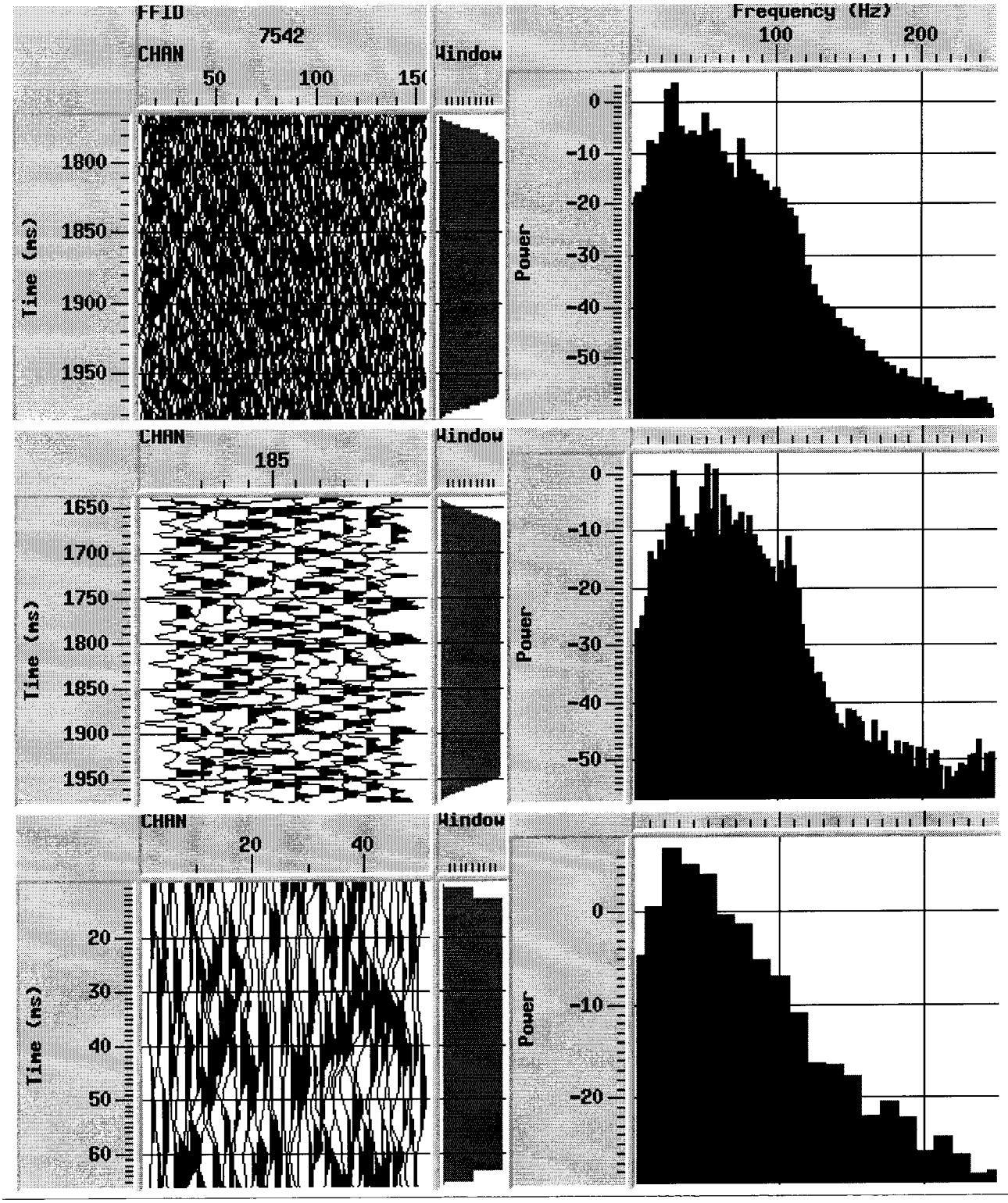

Figure 61. Three power spectra for the subtraction record of Figure 60.

Note: The spectra (right-hand panels) are produced from data shown in left-hand panels, which are portions of the complete data panel of Figure 60. These illustrate the band-limited correlation noise.

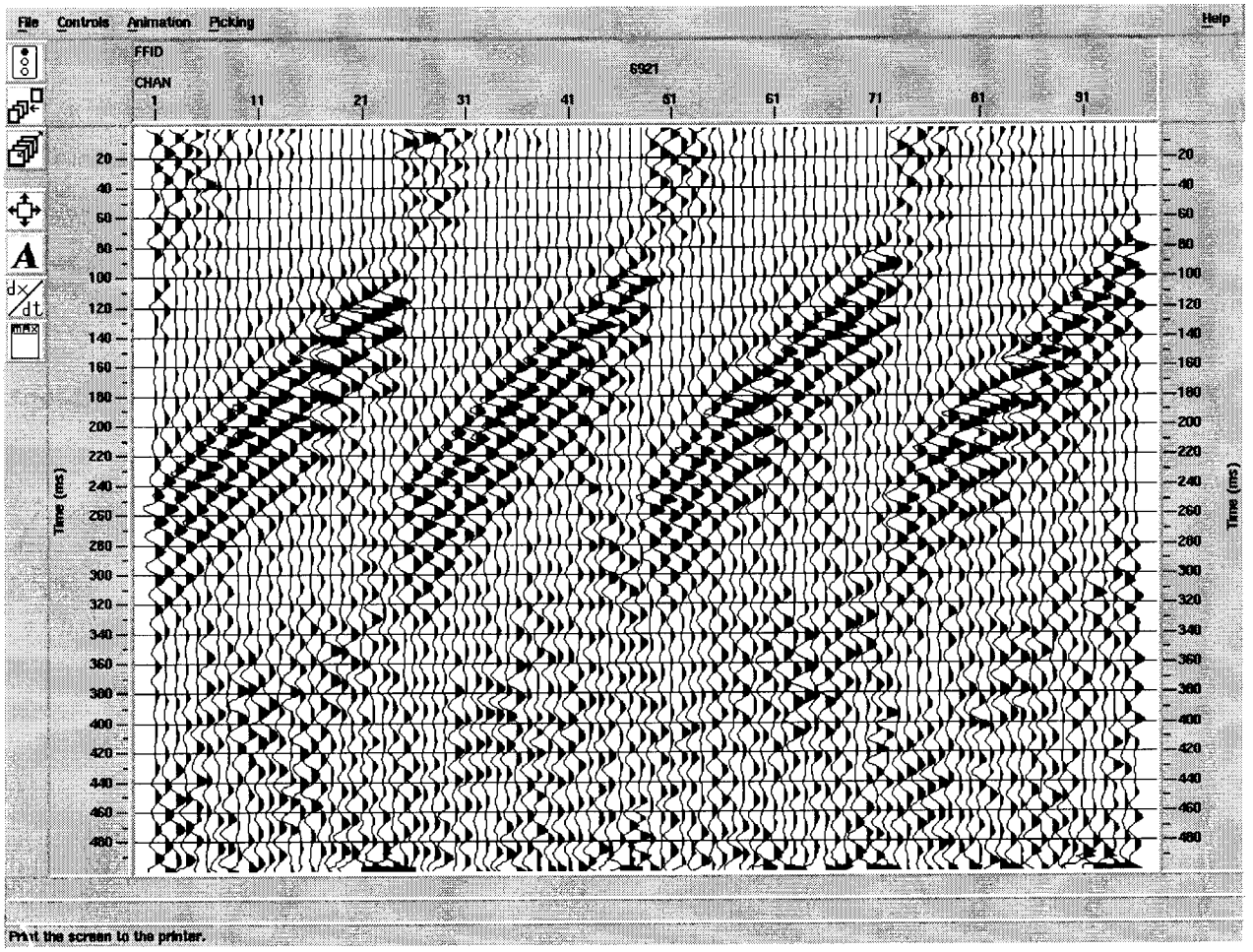

Figure 62. Filtered shot panel, VP 5426, 1 sweep.

Note: Only 4 receiver lines (channels 1-96) are shown. A 50 Hz high-pass filter has been applied. Source array - 2 vibrators.

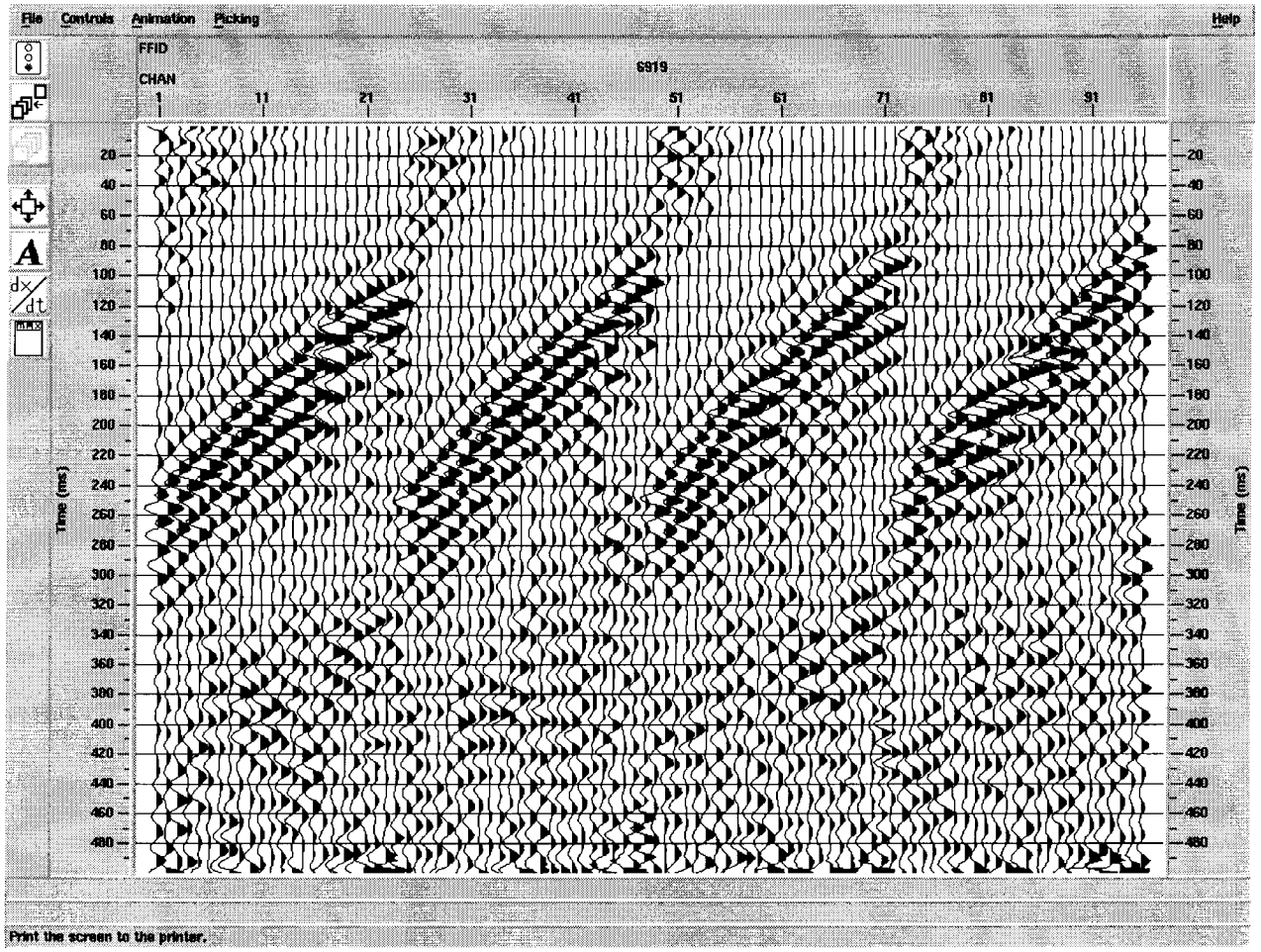

Figure 63. Filtered shot panel, VP 5426, 5 sweeps summed.

Note: Only 4 receiver lines (channels 1-96) are shown. A 50 Hz high-cut filter has been applied. Source array - 2 vibrators with 5 m move-up.

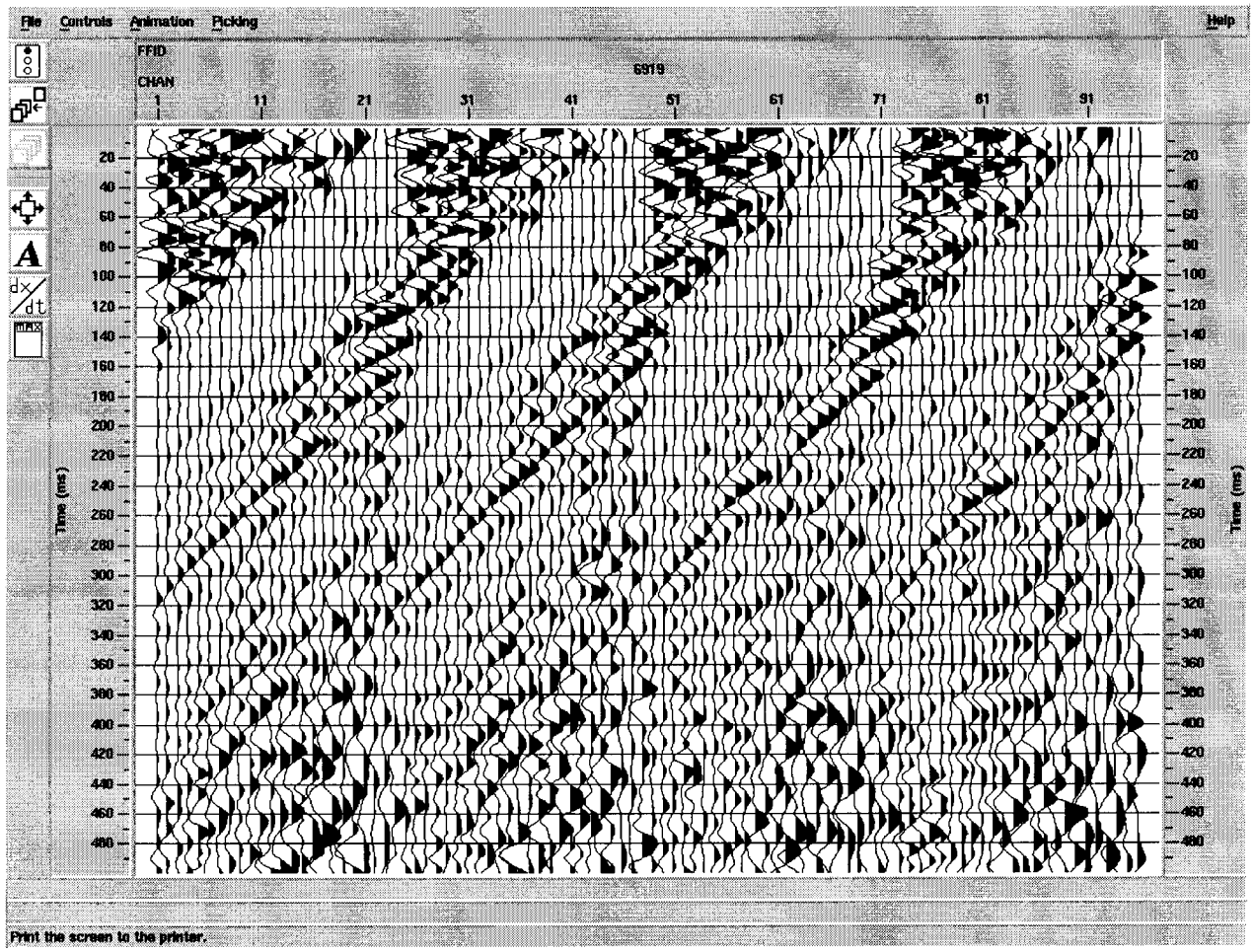

Figure 64. Difference panel, VP 5426.

Note: This is the result of subtracting the panel in Figure 62 (1 sweep) from the data in Figure 63 (5 sweeps summed).

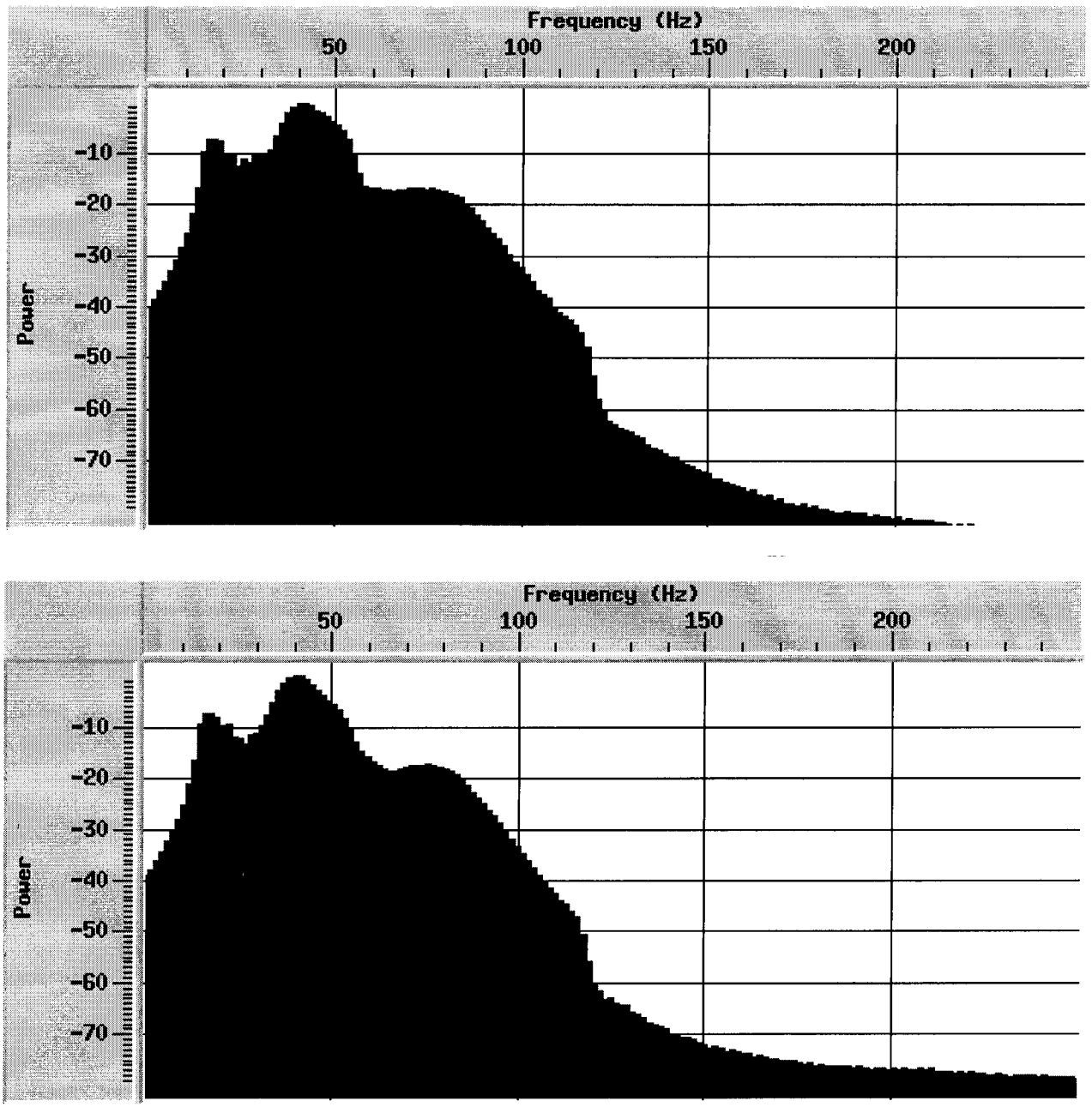

Figure 65. Power spectra for VP 5426; no high-pass filter.

Note: The upper spectrum is for the single sweep (whole panel shown in Figure 62). The lower spectrum is for the 5-sweep sum (Figure 63).

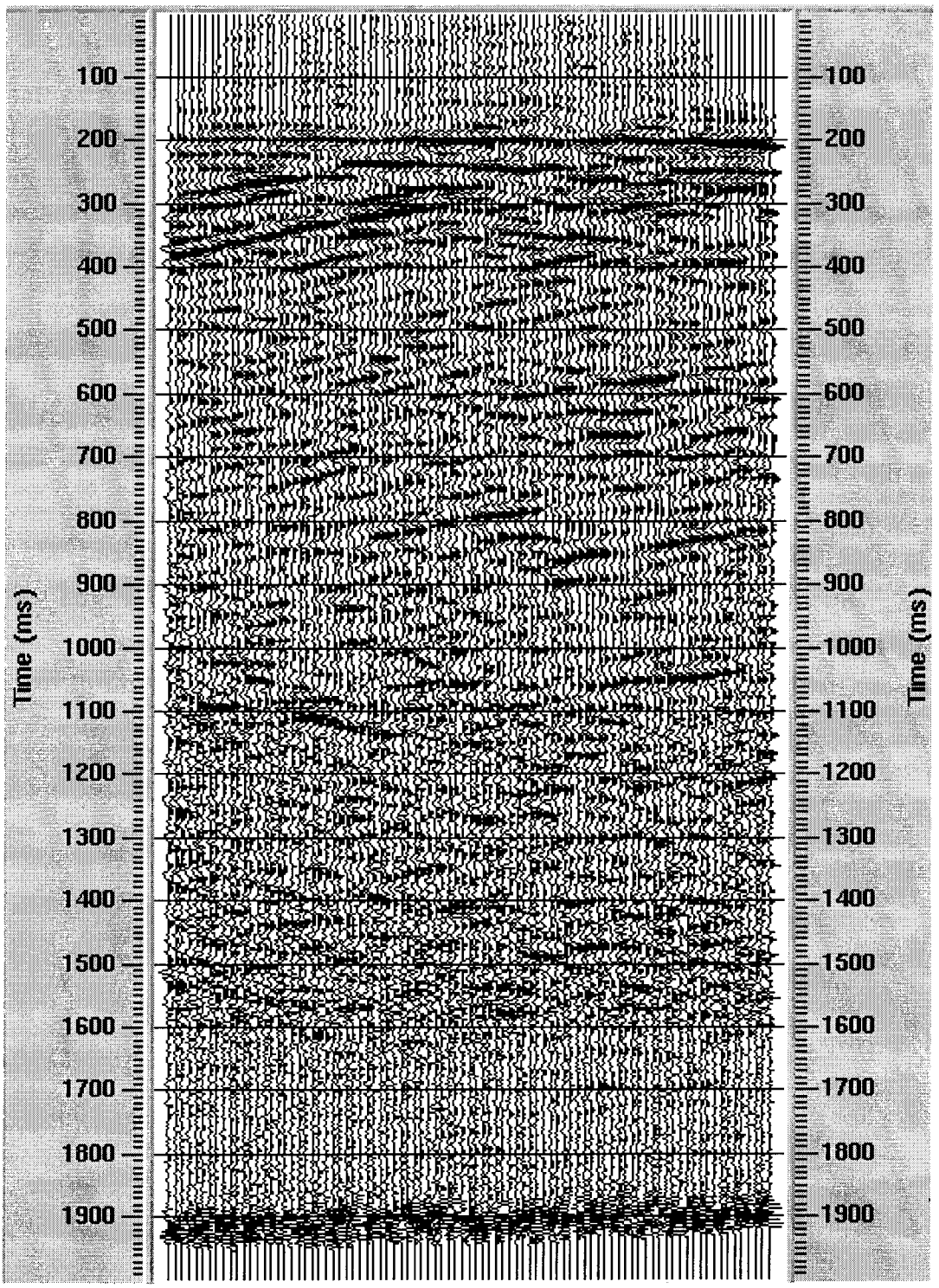

Figure 66. Unfiltered display of crossline X30 (Res2 stack with FXY and FK).

Note: Orientation is NW-SE with NW on the right.

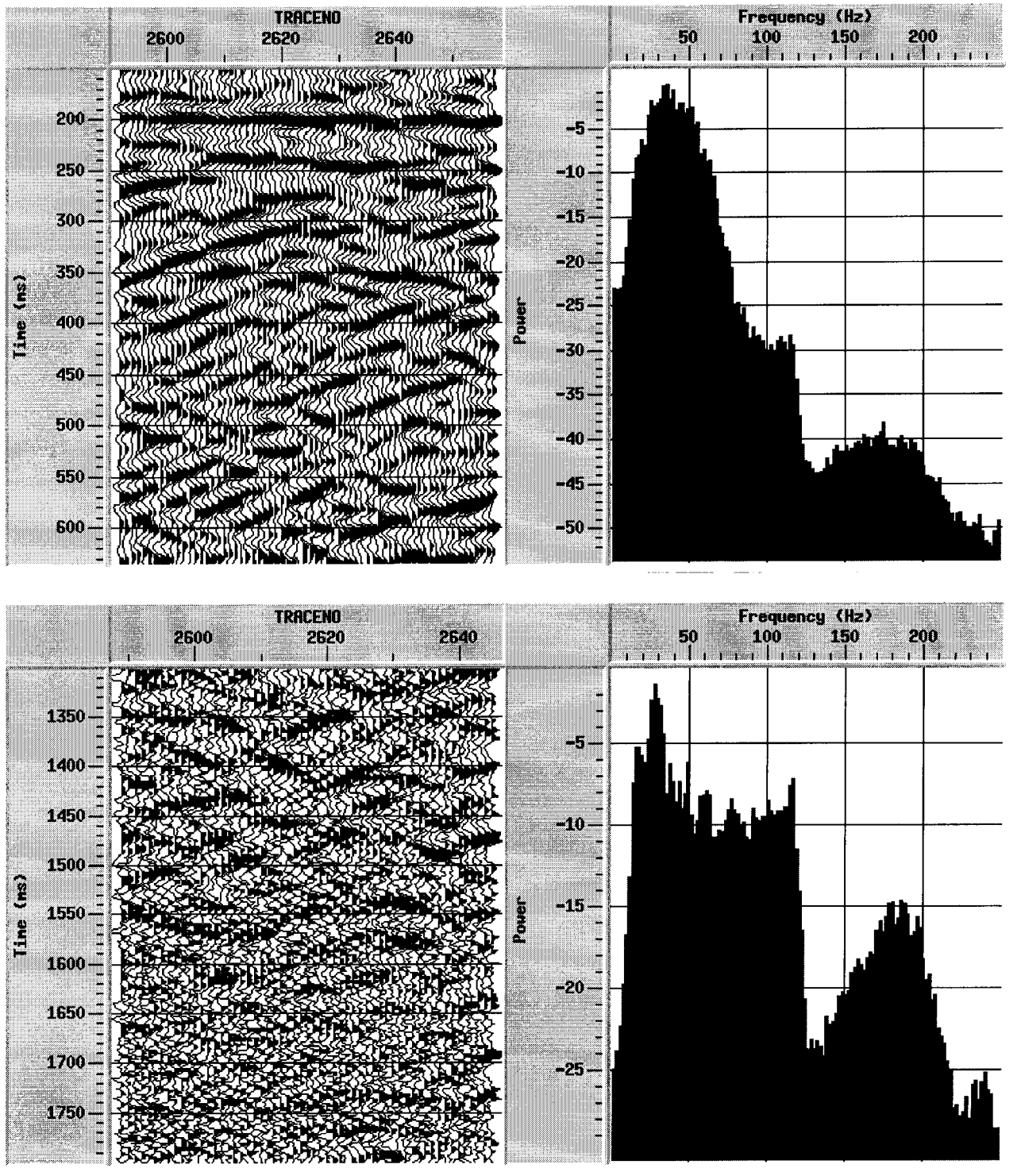

Figure 67. Frequency power spectra for portions of crossline X30 in Figure 66.

Note: Upper row shows spectrum of an area of strong reflections. Lower row depicts the spectrum of an area of low signal.

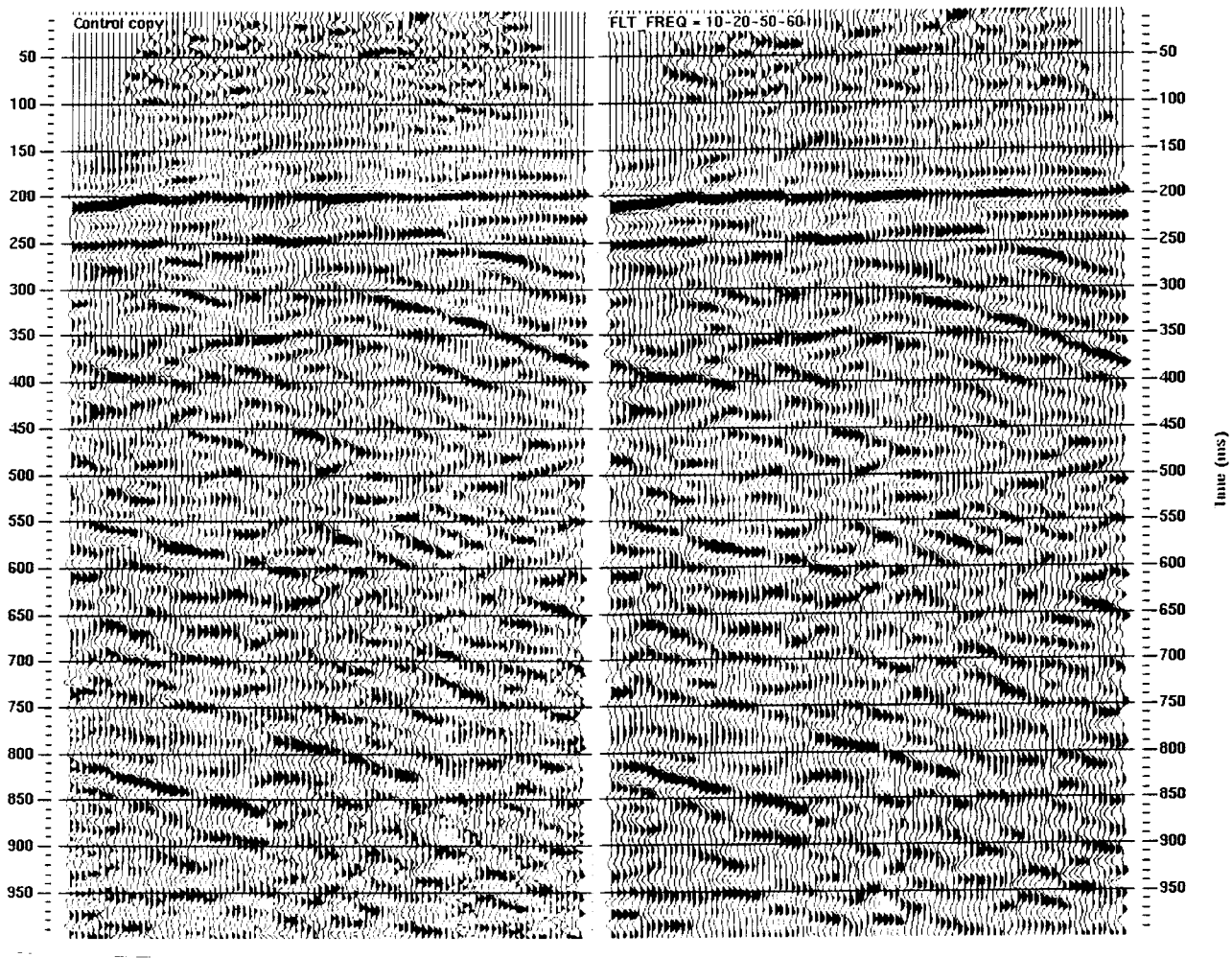

Unfiltered

20-50 Hz

Figure 68. Filter test panels for crossline X30: Unfiltered and 20-50 Hz.

Note: Line is displayed with NW on the left.

.

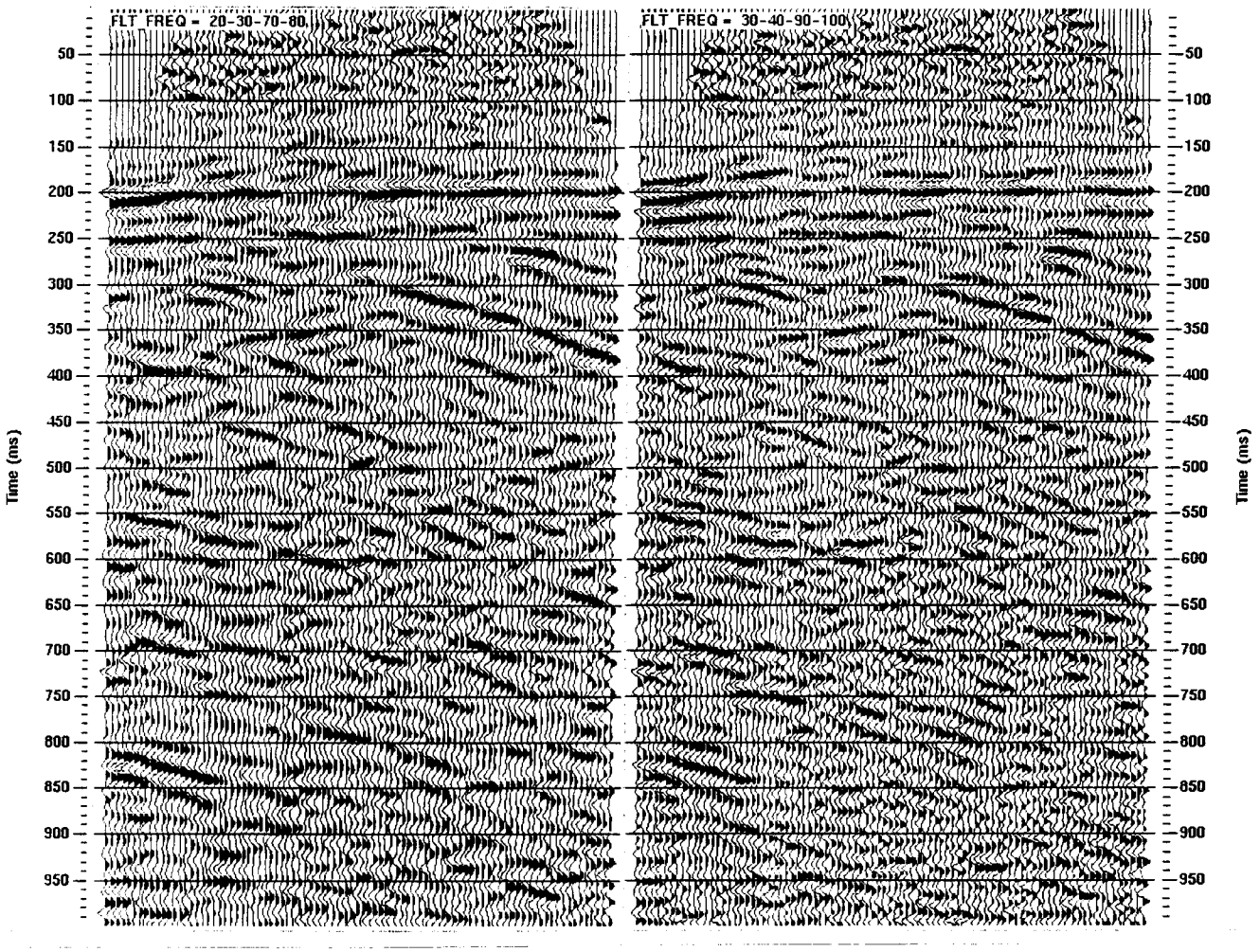

30-70 Hz

40-90 Hz

Figure 69. Filter test panels for crossline X30: 30-70 and 40-90 Hz.

Note: Line is displayed with NW on the left.

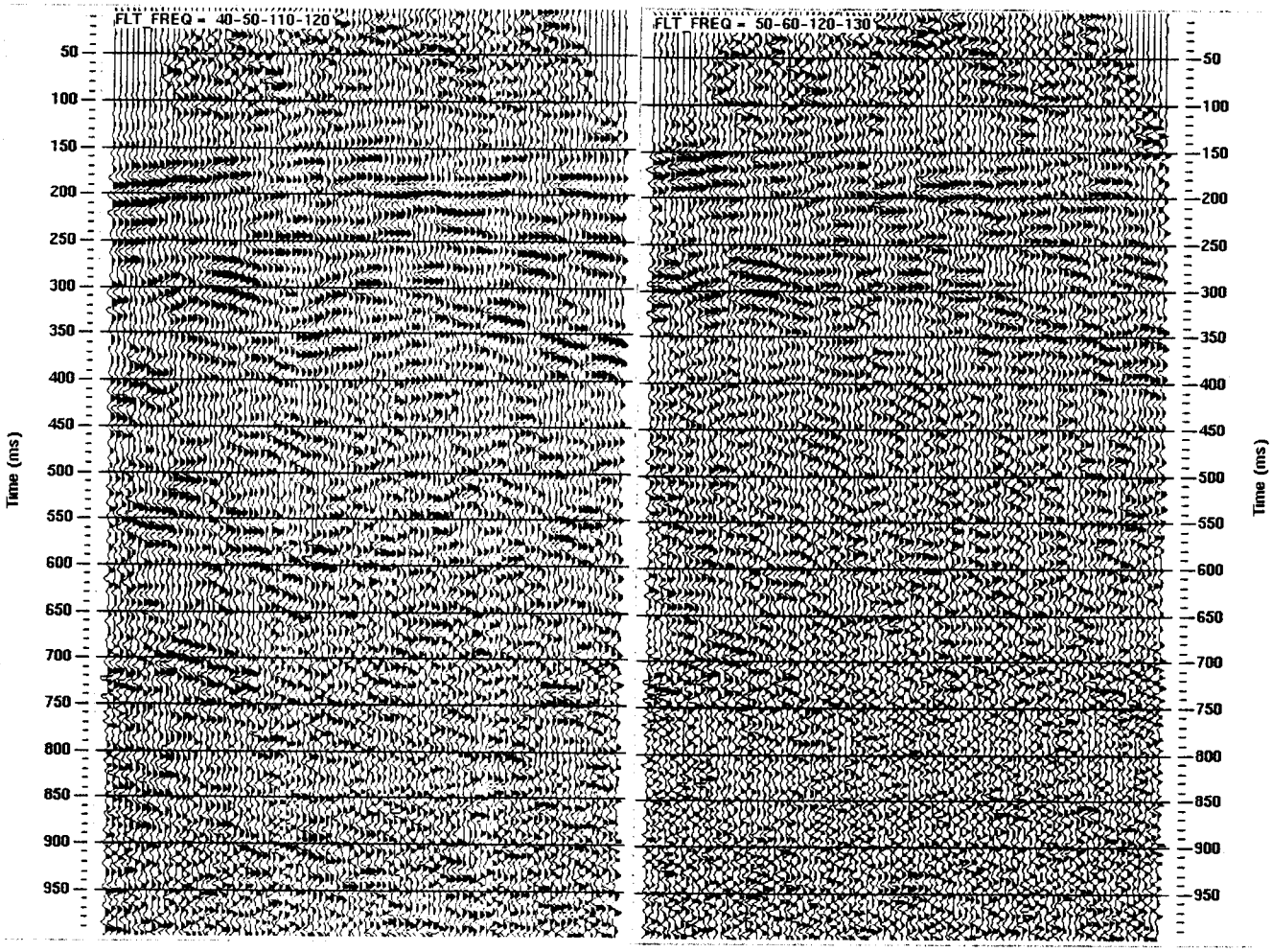

50-110 Hz

60-120 Hz

Figure 70. Filter test panels for crossline X30: 50-110 and 60-120 Hz.

Note: Line is displayed with NW on the left.

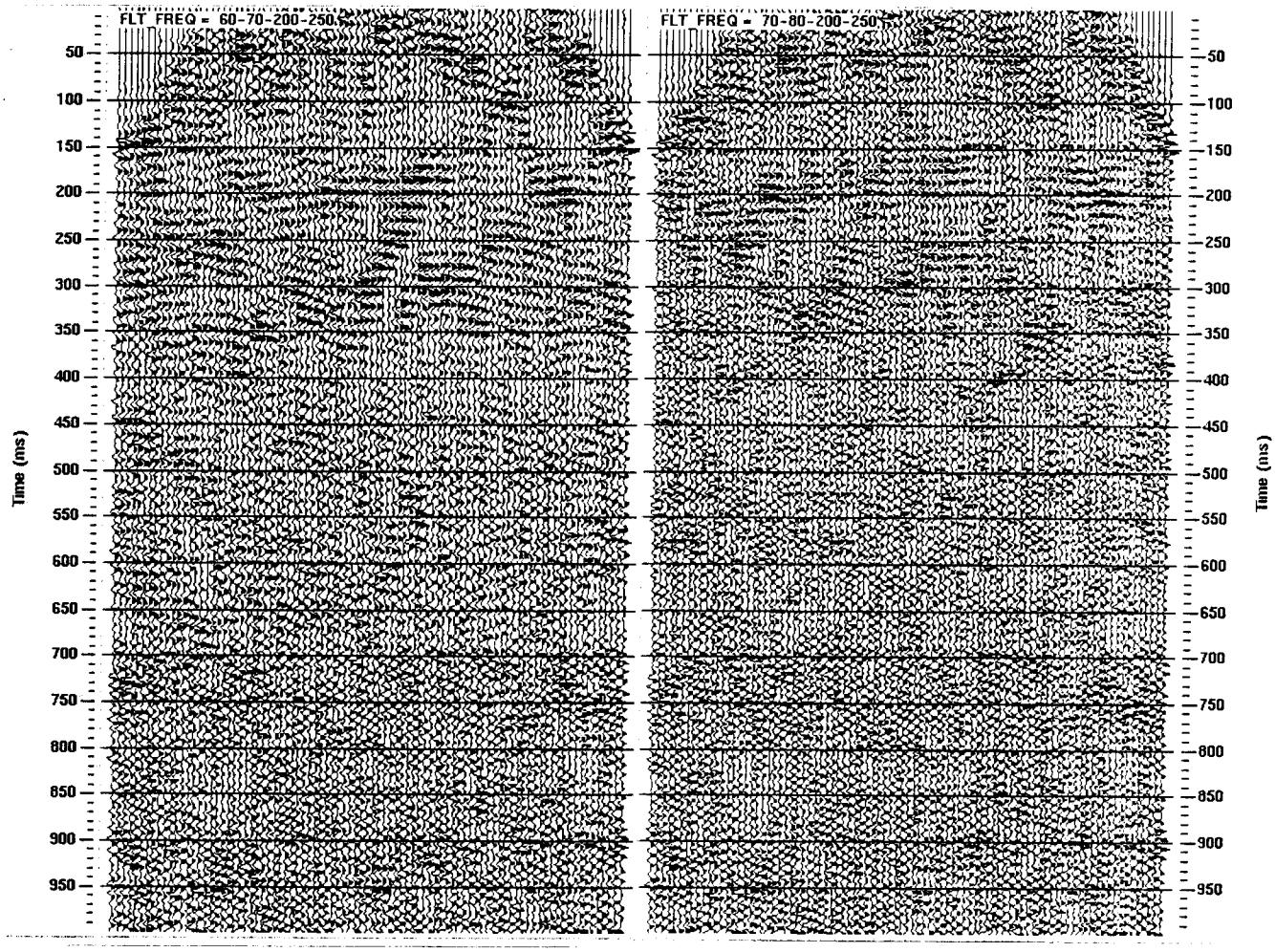

70-200 Hz

80-220 Hz

Figure 71. Filter test panels for crossline X30: 70-200 and 80-200 Hz.

Note: Line is displayed with NW on the left.

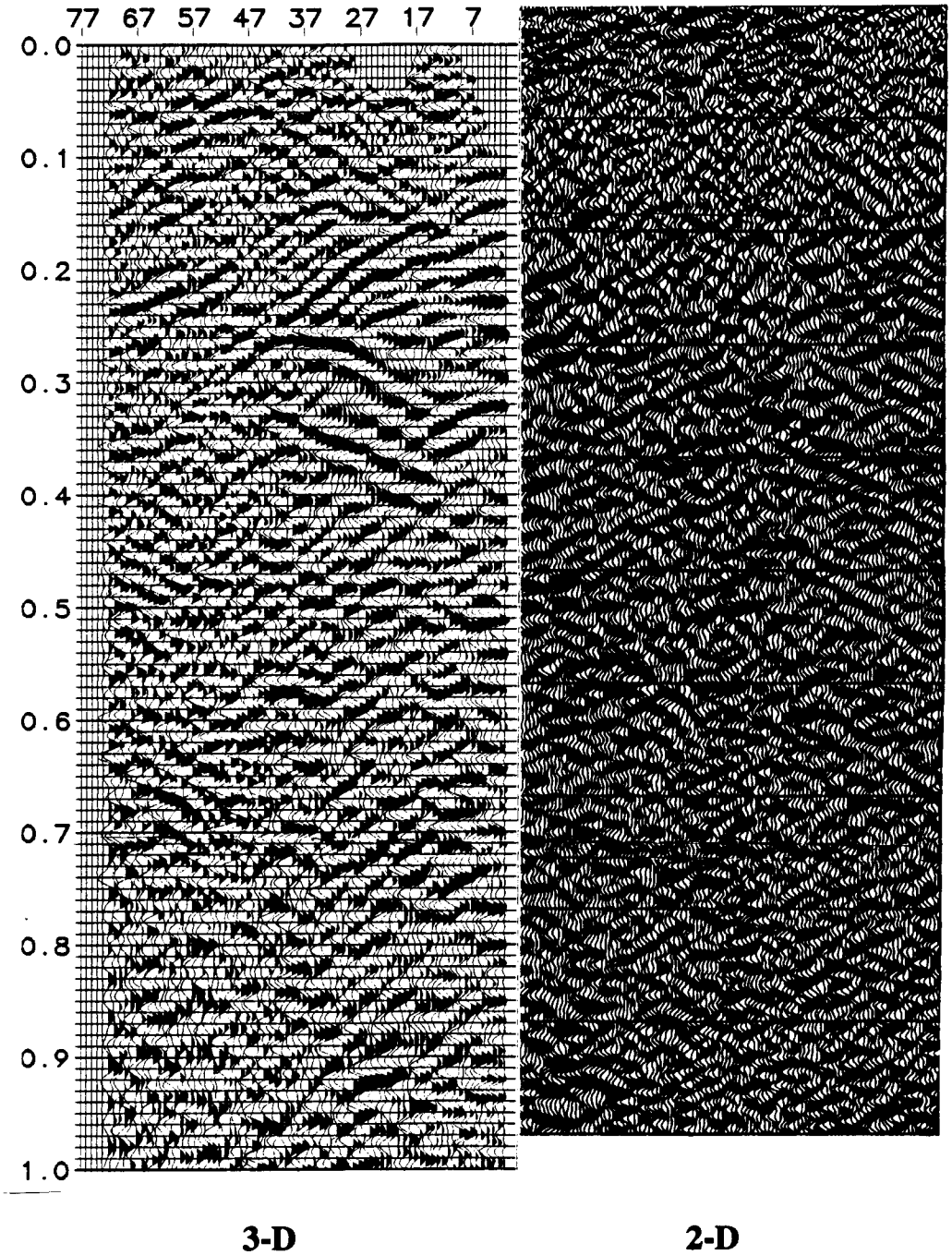

Figure 72. Comparison of inline I13 and 92-2D-05 at the same scale.

Note: A 30 ms static shift has been applied to the 2-D line to match the 3-D data.

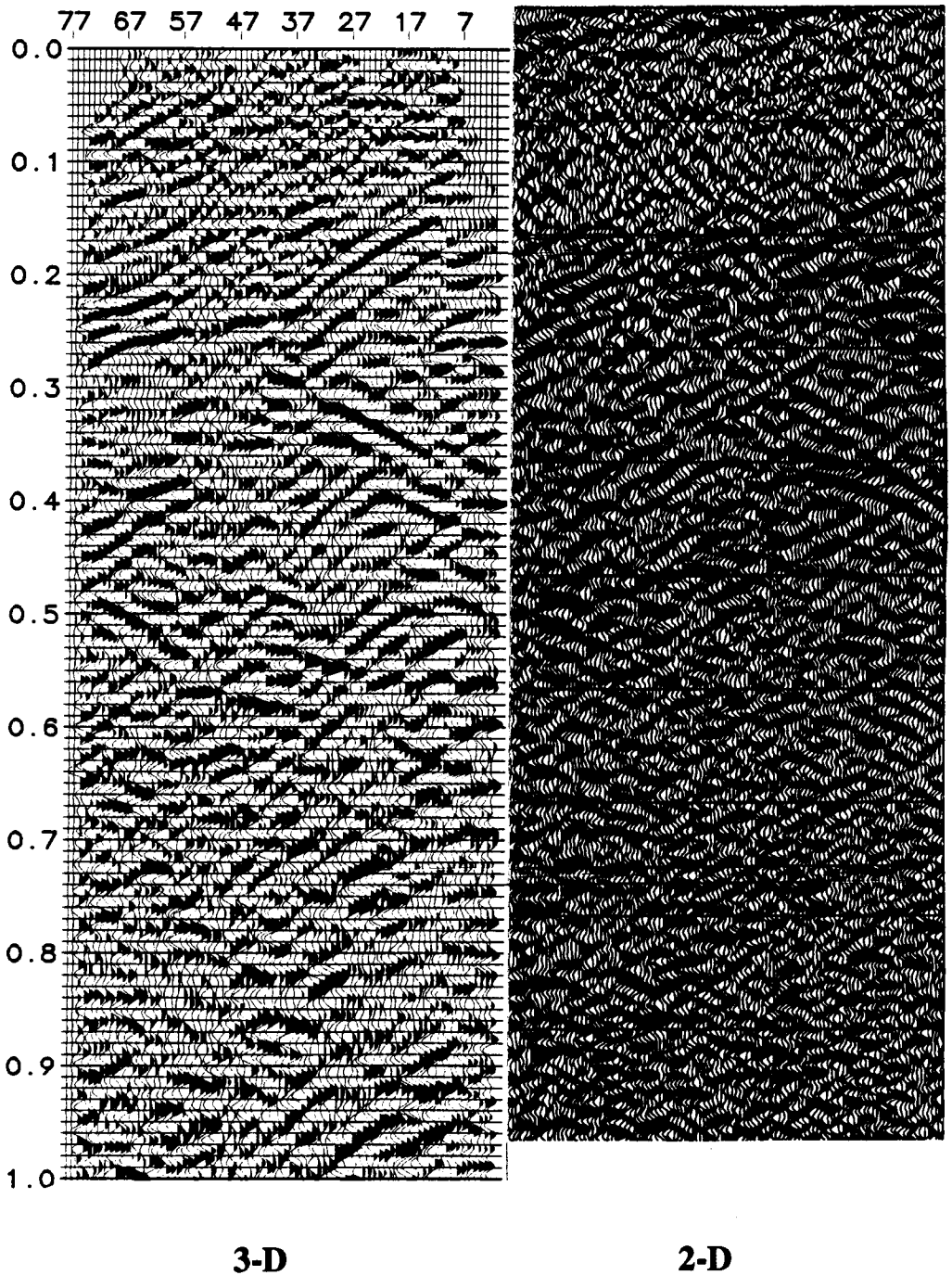

Figure 73. Comparison of inline I32 and 92-2D-04 at the same scale.

Note: A 30 ms static shift has been applied to the 2-D line to match the 3-D data.

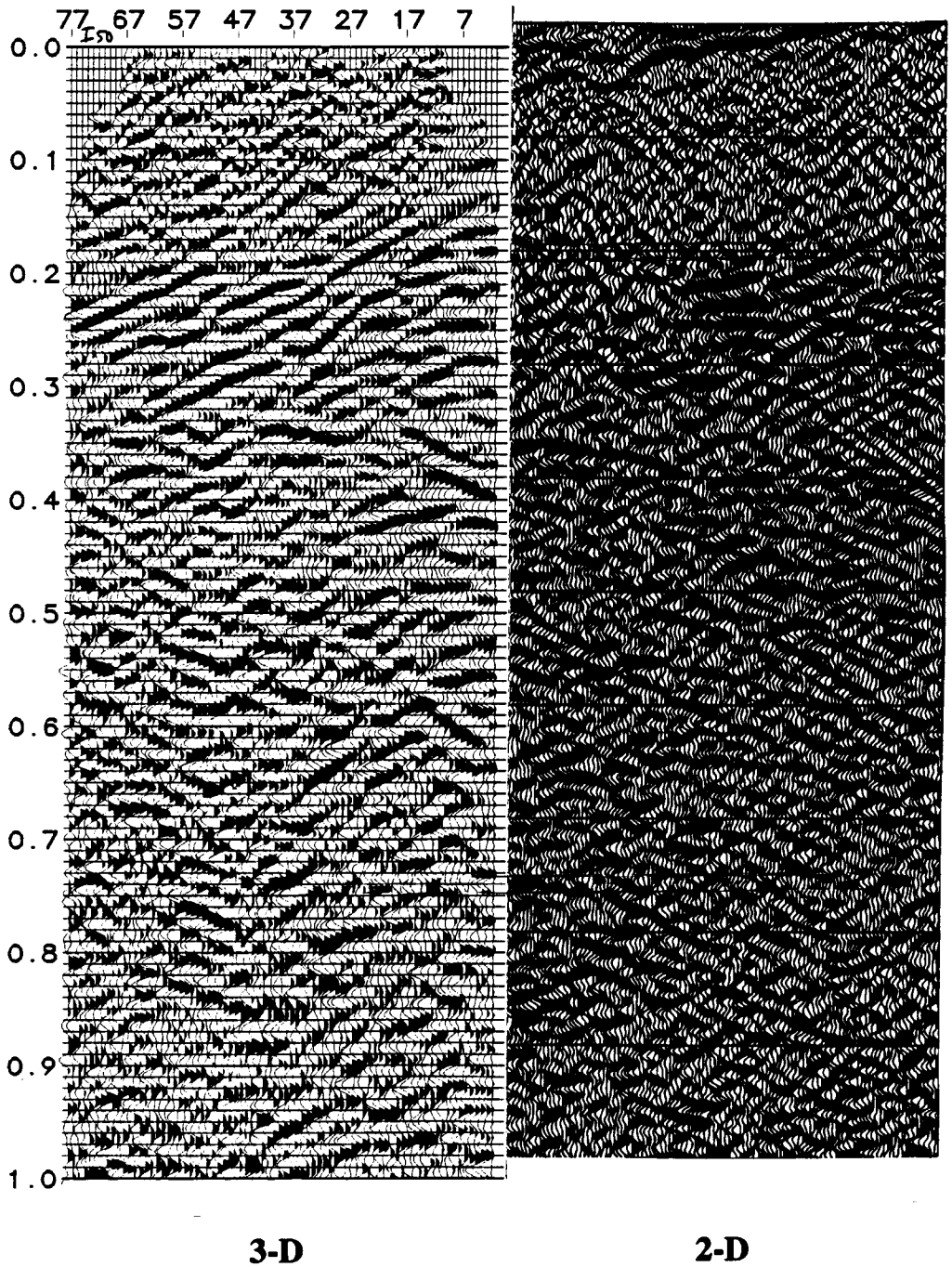

Figure 74. Comparison of inline I50 and 92-2D-03 at the same scale.

Note: A 30 ms static shift has been applied to the 2-D line to match the 3-D data.

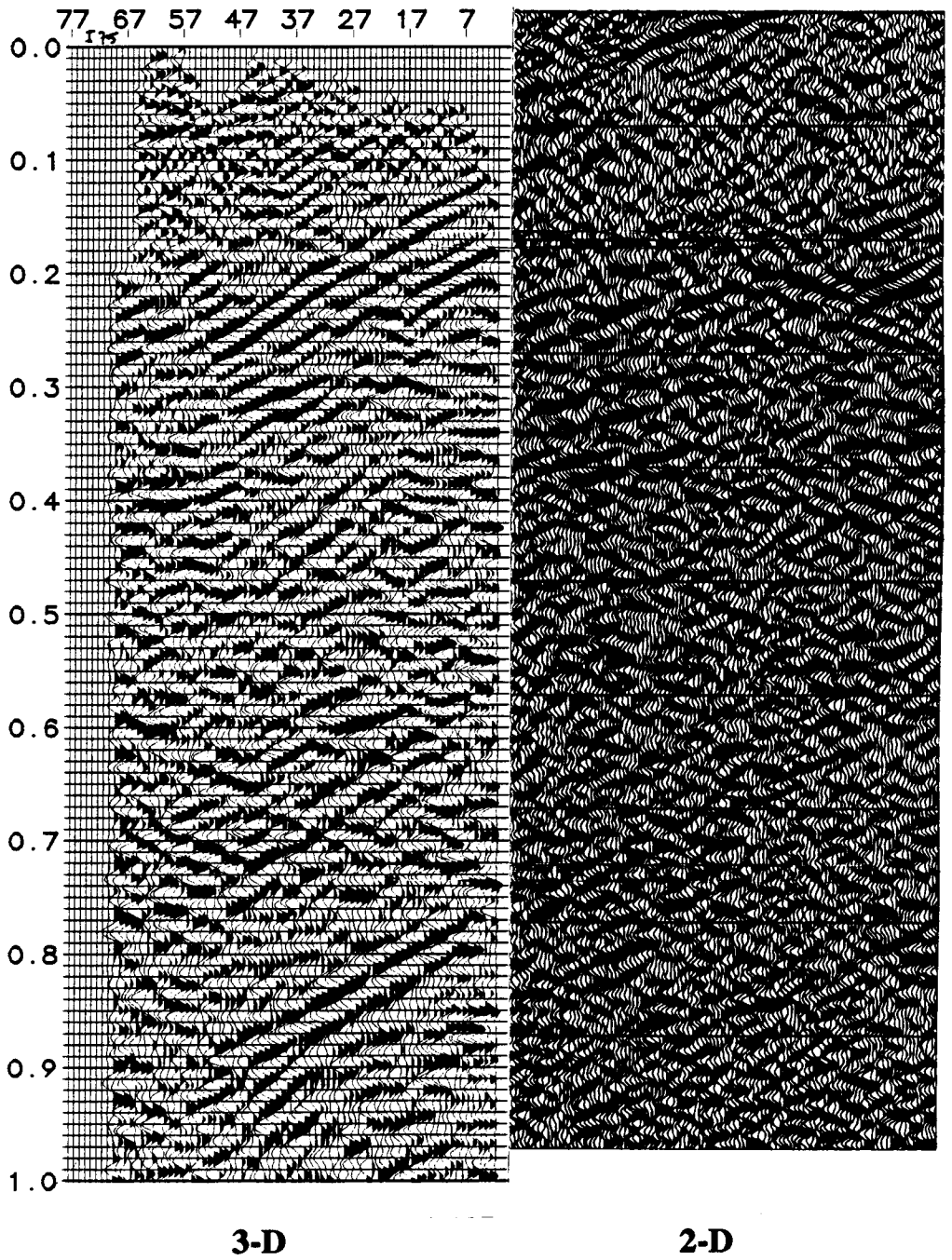

Figure 75. Comparison of inline I75 and 92-2D-02 at the same scale.

Note: A 30 ms static shift has been applied to the 2-D line to match the 3-D data.

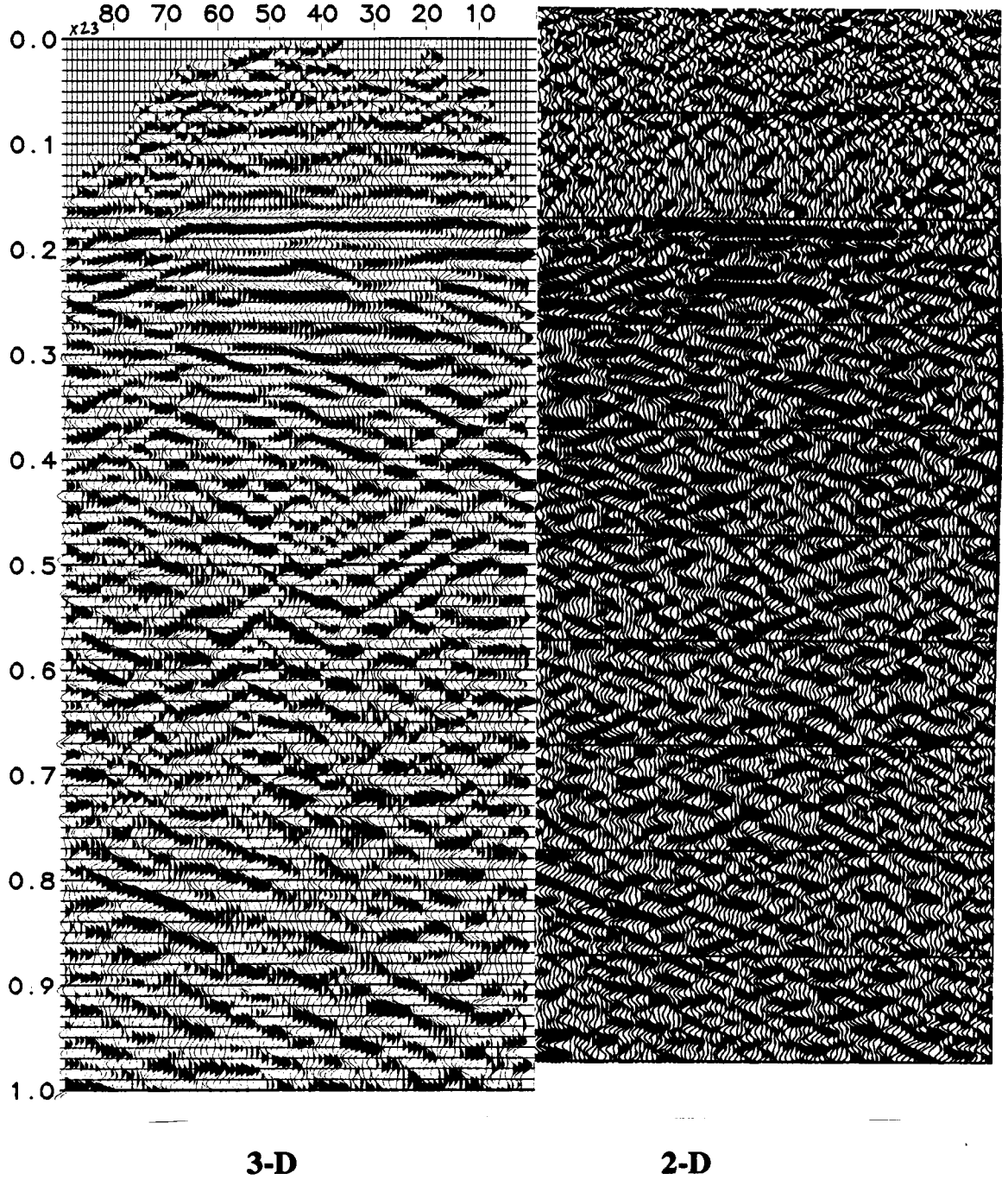

Figure 76. Comparison of crossline X23 and 92-2D-14 at the same scale.

Note: A 30 ms static shift has been applied to the 2-D line to match the 3-D data.

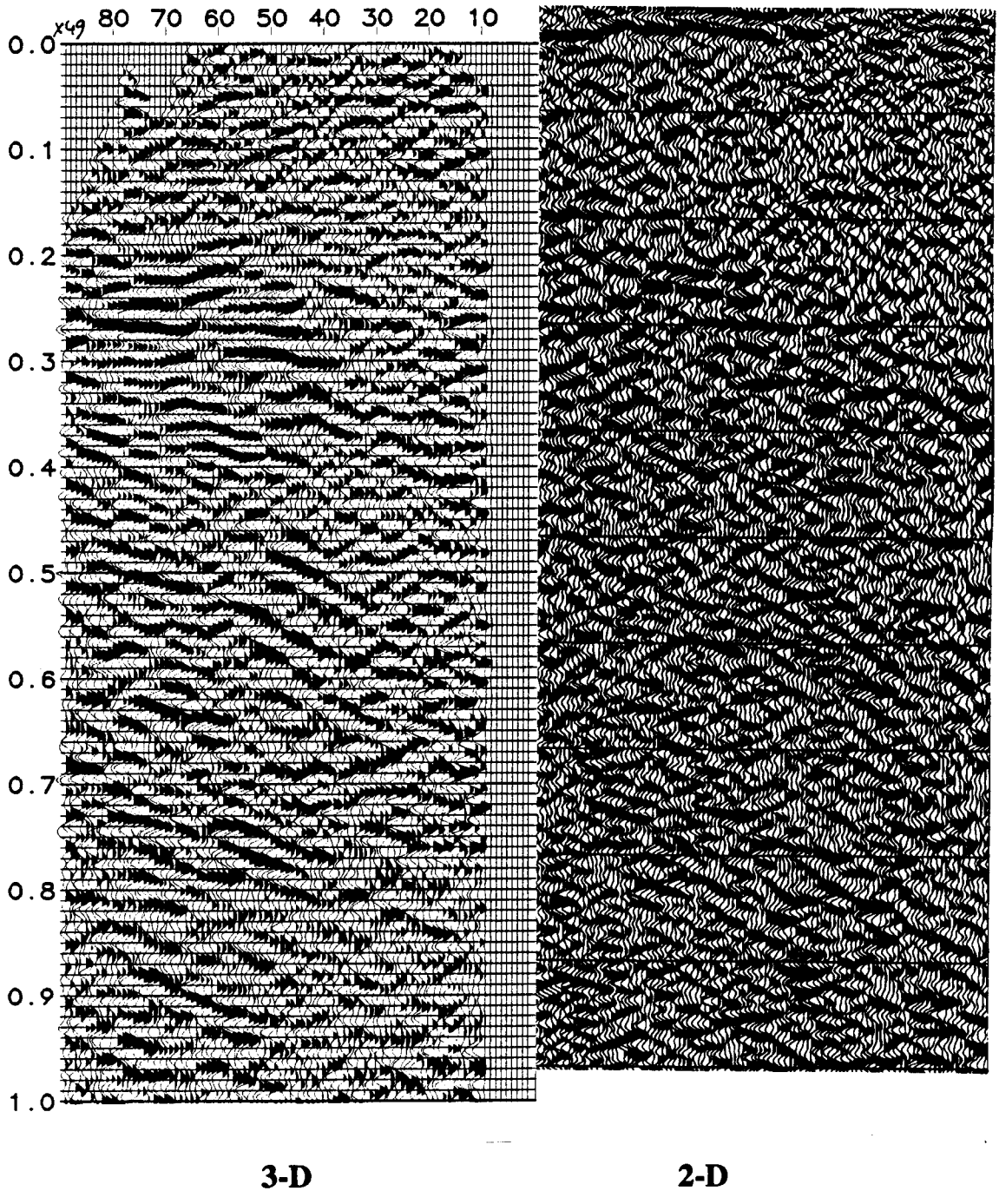

Figure 77. Comparison of crossline X49 and 92-2D-15 at the same scale.

Note: A 30 ms static shift has been applied to the 2-D line to match the 3-D data.